

Cation Distribution in $(M',M)_3\text{Se}_4$

I. $(\text{Cr,Ti})_3\text{Se}_4$

A. HAYASHI, Y. UEDA, AND K. KOSUGE

Department of Chemistry, Faculty of Science, Kyoto University, Kyoto, Japan

H. MURATA AND H. ASANO

Institute of Materials Science, University of Tsukuba, Sakura-mura, Niihari-gun, Ibaraki, Japan

N. WATANABE

National Laboratory for High Energy Physics, Oho-machi, Tsukuba-gun, Ibaraki, Japan

AND F. IZUMI

National Institute for Research in Inorganic Materials, Sakura-mura, Niihari-gun, Ibaraki, Japan

Received May 7, 1986; in revised form August 7, 1986

The cation distribution to the two crystallographic cation sites of the Cr_3S_4 structure was determined in CrTi_2Se_4 and TiCr_2Se_4 by the high-resolution neutron diffraction, using Rietveld analysis. The result showed that the Cr ions preferentially occupy the 2(a) sites. The magnetic properties of the $(\text{Cr,Ti}_{1-x})_3\text{Se}_4$ system were also measured and discussed in relation to the selective substitution of metal ions resulting from the site preference of each ion. © 1987 Academic Press, Inc.

Introduction

In a transition metal (M)—chalcogen (X) system $\text{MX}—\text{MX}_2$, a number of vacancy-ordered phases appear. Among them, the M_3X_4 phase with the Cr_3S_4 structure is of interest because it has been found in so many $M—X$ systems (1, 2) and also shows various physical properties depending on M and X .

The Cr_3S_4 structure¹ (Fig. 1) can be described as the defective NiAs structure which consists of hexagonal close packing of chalcogen atoms with the metal atoms

¹ For the Cr_3S_4 -type structure, an unreduced unit cell with monoclinic space group $I2/m$ has been used for convenience in comparison with the basic NiAs structure. In this paper, however, we chose a reduced unit cell with monoclinic space group $B2/m$ for the Rietveld analysis described later.

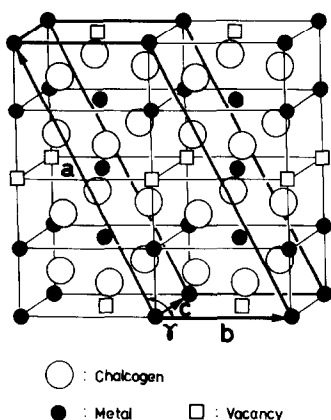


FIG. 1. Cr_3S_4 structure. The thick solid line represents a unit cell for the space group $B2/m$.

occupying the octahedral interstices. In contrast to the NiAs structure, the vacancies are confined to alternate metal layers and ordered within these layers. Therefore, there are two kinds of sites for metal atoms in the structure: one in the half-filled layer ($2(a)$ site), and the other in the fully occupied layer ($4(i)$ site). The structure is referred to, hereafter, as $(M)[M_2]X_4$, where parentheses and brackets denote the half- and the fully occupied layers, respectively.

Not only single metal compounds M_3X_4 , but also a number of mixed-metal compounds $M'M_2X_4$ with the Cr_3S_4 structure, have been reported (3-5). For these $M'M_2X_4$ compounds, it arises as an interesting problem whether or not a metal-ordered structure or a trend of the site preference exists, in addition to a vacancy-ordered structure. Chevreton and Andron reported two types of metal-ordered structures (6):

- (i) normal-type, $(M')[MM]X_4$;
- (ii) inverse-type, $(M)[M'M]X_4$.

The determination of the cation distribution for these compounds is indispensable not only for understanding their diverse physical properties, but also for obtaining information about the nature of chemical bond-

ing. Though there have been several investigations of this problem by means of neutron diffraction, Mössbauer spectroscopy, etc. (7-13), they are restricted to several compounds, and no systematic study varying M' and M has been done so far. We proposed in the previous communication (14) that the investigation of the pseudo-binary system $(M'_xM_{1-x})_3X_4$ serves as a useful tool for this purpose, because the site preference of M and M' should reflect on the compositional dependence of some physical property. In particular, the selenide system $(M'_xM_{1-x})_3\text{Se}_4$ ($M, M' = \text{Ti}, \text{V}, \text{Cr}, \text{Fe}, \text{Co}, \text{and Ni}$) has been chosen because all of the end compounds have the Cr_3S_4 structure. As a part of this investigation, we reported on the phase diagram of solid solution system $(\text{Cr}_x\text{Ti}_{1-x})_3\text{Se}_4$ and the neutron diffraction study of CrTi_2Se_4 (14).

In this paper, we present the results of the cation distribution in CrTi_2Se_4 and TiCr_2Se_4 , determined from the structural refinement using the Rietveld analysis of their high-resolution neutron diffraction patterns. We also report the magnetic properties of the $(\text{Cr}_x\text{Ti}_{1-x})_3\text{Se}_4$ system. The correlation between the cation distribution determined from the Rietveld refinement and the compositional variation of physical properties is discussed.

Experimental

Samples were prepared by direct reaction of the high-purity elements. The details have been reported in our previous communication (14). The phase identification of the samples was made with an X-ray diffractometer using monochromatic $\text{CuK}\alpha$ radiation at room temperature.

Neutron diffraction experiments were carried out with a high-resolution powder diffractometer HRP (15) at KENS pulsed spallation neutron source in the National Laboratory for High Energy Physics. The samples (about 8 g) were placed in a cylin-

drical sample holder (10 mm in diameter) made of vanadium foil which was 25 μm thick. The counting time was about 20 hr.

The magnetic susceptibility was measured from 4.2 K to room temperature using a Faraday-type magnetic torsion balance with an applied field of 8 kOe.

Results

1. Neutron Diffraction Study

HRP adopts a time-of-flight (TOF) technique, in which the sample is irradiated with pulsed white neutrons and the scattered neutrons are detected by backward counters placed at a fixed scattering angle ($2\theta = 170^\circ$). The resolution, $\Delta d/d$, of HRP is about 0.3%, which is superior to that of a conventional double axis diffractometer at a reactor by about one order of magnitude. The diffraction data were analyzed by the Rietveld method (16). In this analysis, the calculated diffraction intensity $Y(t)$ as a function of TOF (t), is expressed as follows (17):

$$Y(t) = Y_s(t) \left[cA(t) \sum_k |F_k|^2 m_k d_k^4 f(\Delta_k) + Y_b(t) \right].$$

In the above equation, $Y_s(t)$ is the incident neutron spectrum, c is the scale factor, $A(t)$ is the absorption correction factor, F_k is the structure factor, m_k is the multiplicity, d_k is the d spacing for k th reflection, and $Y_b(t)$ is the background function. The incident neutron spectrum $Y_s(t)$ has been determined in advance by incoherent scattering of vanadium. The peak shape function $f(\Delta_k)$, where Δ_k is the difference in TOF from the Bragg position of the k th reflection, has been given by Von Dreele *et al.* (17) as a Gaussian resolution function convoluted by rising and decaying exponentials. We modify their expression by adding two asymmetric Lorentzian functions at the peak position and the decaying tail (16), because we em-

ploy a grooved surface moderator which provides more complicated time profile compared to the flat moderator (17). Least-squares refinement is achieved by minimizing the quantity,

$$\sum_i w_i [Y_i(\text{obs}) - Y_i(\text{cal})]^2,$$

where $Y_i(\text{obs})$ and $Y_i(\text{cal})$ are observed and calculated counts for the i th time channel and w_i is a weighting factor.

The assumption made prior to the refinement is that each atom site is completely occupied, that is, no vacancy exists both on metal and selenium sites. This results in the general formula for the cation configuration in the compound $M'M_2X_4$,



where g is the occupation factor of M' for the 2(a) site, which is the only parameter to be refined concerning the cation distribution. The occupation factor, g , and the atomic coordinates were refined, together with the overall temperature factor (B) and the unit cell parameters. The final parameters are given in Table I. The observed and calculated profiles of CrTi_2Se_4 and TiCr_2Se_4 are shown in Figs. 2 and 3, respectively. The experimental data are plotted by dots and the vertical markers indicate Bragg positions. The solid curve overlying the data points is a result of the Rietveld analysis described above and the difference ΔY between observed and calculated counts is shown by a series of dots in the bottom.

2. Magnetic Susceptibility

The temperature dependence of the molar magnetic susceptibility (χ_m) for several samples of $(\text{Cr}_x\text{Ti}_{1-x})_3\text{Se}_4$ is shown in Fig. 4. χ_m for all samples except Ti_3Se_4 ($x = 0$) exhibits a temperature dependence.

χ_m for Ti_3Se_4 is paramagnetic and temperature independent (2×10^{-4} emu/mole), indicating Ti_3Se_4 has no localized magnetic

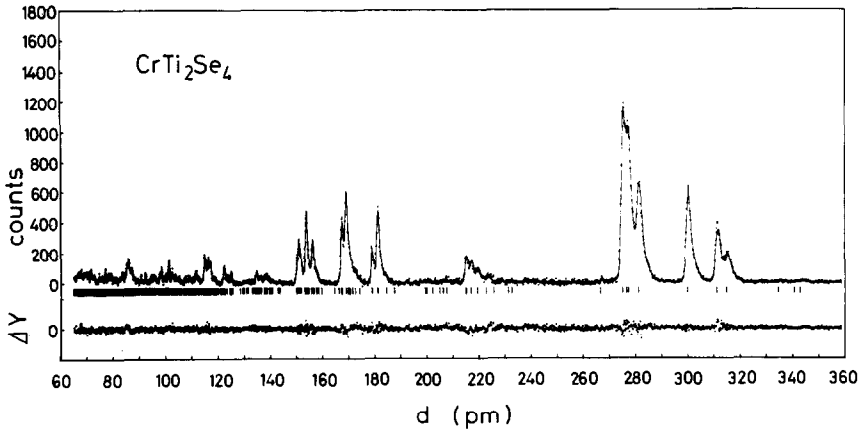

 FIG. 2. Observed (dots) and calculated (solid line) neutron diffraction pattern of CrTi_2Se_4 .

TABLE I
FINAL ATOMIC PARAMETERS FOR CrTi_2Se_4 AND
 TiCr_2Se_4 WITH ESTIMATED STANDARD DEVIATIONS
IN PARENTHESES

CrTi_2Se_4					
Atom	Position	x	y	z	Occupancy
Cr(1)	2(a)	0	0	0	0.694
Ti(1)	2(a)	0	0	0	0.306
Cr(2)	4(i)	0.2548(9)	0.222(2)	0	0.153
Ti(2)	4(i)	0.2548(9)	0.222(2)	0	0.847
Se(1)	4(i)	0.6308(3)	0.2959(7)	0	1.0
Se(2)	4(i)	0.8857(2)	0.2241(6)	0	1.0

$a = 13.6581 \text{ \AA}$; $b = 6.2992 \text{ \AA}$; $c = 3.577 \text{ \AA}$; $\gamma = 118.59^\circ$; $B^a = 0.30(2) \text{ \AA}^2$; $R_{\text{wp}}^b = 8.8\%$; $R_B^c = 4.3\%$

TiCr_2Se_4					
Atom	Position	x	y	z	Occupancy
Ti(1)	2(a)	0	0	0	0.160
Cr(1)	2(a)	0	0	0	0.840
Ti(2)	4(i)	0.269(2)	0.261(7)	0	0.420
Cr(2)	4(i)	0.269(2)	0.261(7)	0	0.580
Se(1)	4(i)	0.6326(2)	0.2940(7)	0	1.0
Se(2)	4(i)	0.8834(2)	0.2189(6)	0	1.0

$a = 13.5541 \text{ \AA}$; $b = 6.2913 \text{ \AA}$; $c = 3.5871 \text{ \AA}$; $\gamma = 119.01^\circ$; $B^a = 0.49(2) \text{ \AA}^2$; $R_{\text{wp}}^b = 8.7\%$; $R_B^c = 3.9\%$.

^a B : overall temperature factor.

$$^b R_{\text{wp}} = \left[\sum_i w_i \{Y_i(\text{obs}) - Y_i(\text{cal})\}^2 / \sum_i w_i \{Y_i(\text{obs})\}^2 \right]^{1/2}.$$

$$^c R_B = \sum_k \left| I_k(\text{obs}) - I_k(\text{cal}) \right| / \sum_k I_k(\text{obs}). \quad (I_k(\text{obs}) \text{ and } I_k(\text{cal}) \text{ are observed and calculated integrated intensities for the } k\text{th reflection.})$$

$I_k(\text{cal})$ are observed and calculated integrated intensities for the k th reflection.)

moment. Compounds having $x = 1.0$ (Cr_3Se_4) and $x = 0.9$ show a typical antiferromagnetic behavior with $T_N = 82$ and 38 K, respectively. The value of $T_N = 82$ K for Cr_3Se_4 is in good agreement with that reported by Bertaut *et al.* (18) and by Yuzuri (19). For $0.4 \leq x \leq 0.8$, χ_m shows a broad maximum around 10 K suggesting some kind of magnetic ordering.

Above about 77 K, χ_m for all samples but Ti_3Se_4 obeys a Curie-Weiss law: $\chi_m = C_m / (T - \theta) + \chi_0$, where C_m is the molar Curie constant, θ is the Weiss constant, and χ_0 is the temperature-independent susceptibility. χ_0 is nearly equal to zero for $0.3 \leq x \leq 1$ and the order of χ_m of Ti_3Se_4 for $x = 0.1$ and 0.2 . Figure 5 shows the reciprocal susceptibility $1/(\chi_m - \chi_0)$ vs temperature (T) curves. Figure 6 shows the compositional dependence of the parameters C_m and θ , calculated from the slope and the intercept of the $1/(\chi_m - \chi_0)$ vs T curves in Fig. 5. C_m increases linearly with x but the slope of the C_m vs x curve changes above $x = 0.7$. In the $(\text{Cr}_x\text{Ti}_{1-x})_3\text{Se}_4$ system, it seems reasonable that the Ti atoms have no magnetic moment and C_m is a measure of the localized magnetic moment of the Cr ions. Figure 7 shows the compositional dependence of the effective number of Bohr magnetons, P_{eff} ,

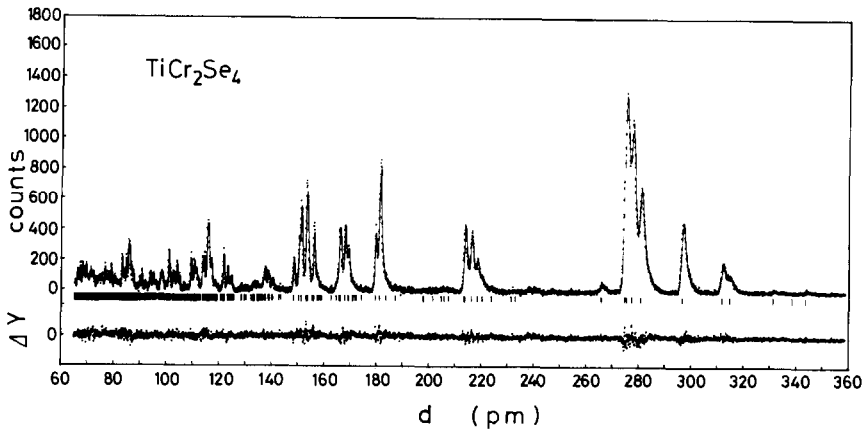


FIG. 3. Observed (dots) and calculated (solid line) neutron diffraction pattern of TiCr_2Se_4 .

per Cr ions. P_{eff} has the constant value of about $4\mu_B$ in the composition range $0 < x < 0.7$ and over $x = 0.7$ increases monotonously to the value of about $4.7\mu_B$ at $x = 1$ (Cr_3Se_4). The value of $4\mu_B$ is close to the one corresponding to the Cr^{3+} ion ($3.87\mu_B$ estimated from d -spin moments only: d^3 , $S = \frac{3}{2}$), while the value for $x = 1$ (Cr_3Se_4) is close to the average moment ($4.21\mu_B$) of Cr^{3+} and Cr^{2+} ions based on an ionic configuration $\text{Cr}^{2+}\text{Cr}_2^{3+}\text{Se}_4^{2-}$ for Cr_3Se_4 .

On the other hand, the Weiss constant θ

increases with increasing x , showing a maximum value of 56 K around $x = 0.3$, and then decreases to the value of -48 K for Cr_3Se_4 ($x = 1$), changing its sign from positive to negative at about $x = 0.8$. The value of $\theta = -48$ K for Cr_3Se_4 seems to be reasonable for the antiferromagnetic compounds with $T_N \approx 80$ K. The change of sign of θ from positive to negative means the change of predominant magnetic interactions from ferromagnetic to antiferromagnetic.

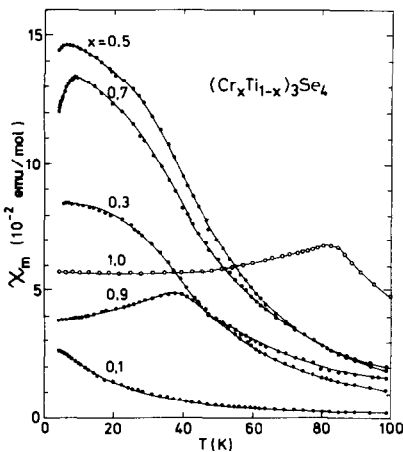


FIG. 4. Temperature dependence of molar magnetic susceptibility of the samples of $(\text{Cr}_x\text{Ti}_{1-x})_3\text{Se}_4$.

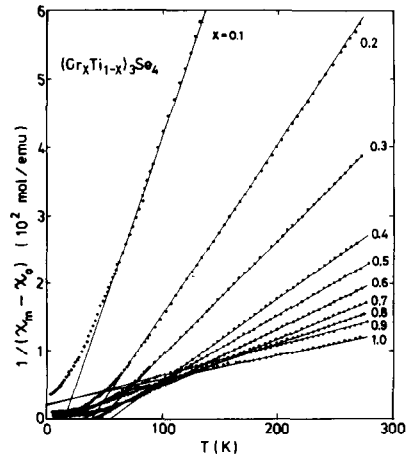


FIG. 5. Plot of the inverse magnetic susceptibility, $1/(\chi_m - \chi_0)$ vs temperature for the samples of $(\text{Cr}_x\text{Ti}_{1-x})_3\text{Se}_4$.

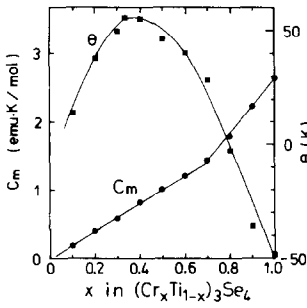
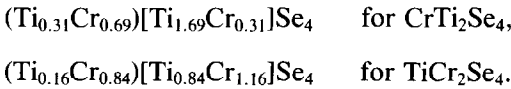


FIG. 6. Composition dependence of the Curie constant (solid circles) and Weiss constant (solid squares).

Discussion

As presented in Table I, the Rietveld analysis resulted in the following cation distribution:



These results reveal that CrTi_2Se_4 and TiCr_2Se_4 have approximately the normal- and inverse-type metal-ordered structure, respectively. The normal-type configuration for CrTi_2Se_4 is also consistent with the results of a preliminary neutron study (14). Therefore, we can say that the Cr ions have a tendency to occupy the 2(a) site relative to the Ti ions.

CrTi_2Se_4 and TiCr_2Se_4 are compounds appearing at $x = \frac{1}{3}$ and $\frac{2}{3}$ in a pseudo-binary

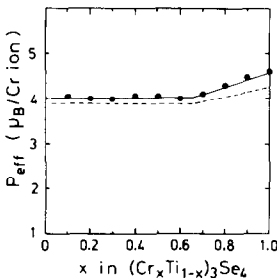


FIG. 7. Composition dependence of the effective number of Bohr magnetons per Cr ion. A broken line was obtained from the present assumption (see text).

system $(\text{Cr}_x\text{Ti}_{1-x})_3\text{Se}_4$, respectively. For a pseudo-binary solid solution $(M'_xM_{1-x})_3\text{Se}_4$ system, we have hypothesized three simplified modes for the substitution based on the site preference of each metal (14):

(A) M' substitutes for M in the 2(a) sites preferentially.

(B) M' substitutes for M in the 4(i) sites preferentially.

(C) Neither M' nor M has a preference for either site.

It can be expected that an anomalous change in the compositional dependence of physical properties should appear at the composition $x = \frac{1}{3}$ for case (A), and $x = \frac{2}{3}$ for case (B).

As we have already reported (14), the compositional variation of the lattice parameters (Fig. 8) has a turning point at around $x = \frac{1}{3}$ (CrTi_2Se_4) showing the deviation from Vegard's law. Furthermore, we have observed a minimum in the variation of the phase transition temperature (T_1) at the same composition, $x = \frac{1}{3}$ (14).

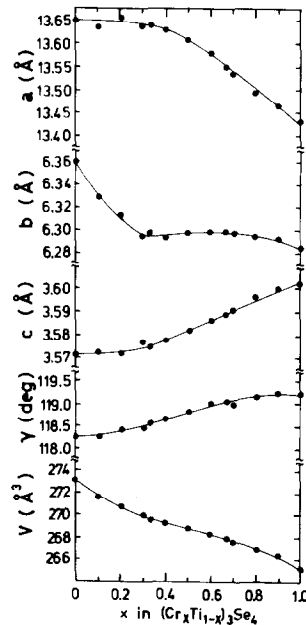


FIG. 8. Composition dependence of the lattice parameters (a , b , c , and γ) and unit cell volume (V).

These results reveal that the substitution mode in $(\text{Cr}_x\text{Ti}_{1-x})_3\text{Se}_4$ is case (A), that is, the Cr ions have the site preference for the 2(a) sites, and accordingly the normaltype CrTi_2Se_4 at $x = \frac{1}{3}$ and the inversetype TiCr_2Se_4 at $x = \frac{2}{3}$ are formed. The results of the Rietveld analyses on the compounds CrTi_2Se_4 and TiCr_2Se_4 support our simplified model for the substitution, where the substitution proceeds according only to the site preference of each metal over the whole composition range of the system.

Next, let us discuss the magnetic properties with regard to the above substitution model. Cr_3Se_4 is an antiferromagnetic compound with $T_N = 80$ K. The spin structure was confirmed by Bertaut *et al.* (18) to be that of ferromagnetic (010) layers coupled antiferromagnetically to each other. As shown in Fig. 1, the metal layer stacking parallel to the (010) plane is expressed as $M^F M^V M^F \square M^F M^V M^F \square \dots$, where M^F denotes the metal layer formed by 4(i)-site metals (metals in a fully occupied metal layer), M^V represents 2(a)-site metals (metals in a half-filled metal layer), and \square signifies a vacancy layer. Therefore, the spin structure is expressed as $M_+^F M_-^V M_+^F \square M_-^F M_+^V M_-^F \square \dots$, where + and - specify spin directions of the interlayer antiferromagnetic coupling. The analysis of magnetic susceptibility measurements for $(\text{Cr}_x\text{Ti}_{1-x})_3\text{Se}_4$ has revealed that only Cr ions are magnetic in this system. In this situation, the observed compositional variation of θ may be understood on the basis of the selective substitution mentioned above. θ is a measure of the two competing magnetic interactions, that is, intralayer ferromagnetic and interlayer antiferromagnetic interactions. Starting from Cr_3Se_4 ($x = 1$), which is an antiferromagnet with $T_N = 82$ K, the selective substitution of Ti for Cr ions in the M^F layer results in the dilution of magnetic ions in the M^F layer with decreasing x for $1 \geq x \geq \frac{1}{3}$, and the magnetic structure $\text{Ti}^F \text{Cr}_+^V \text{Ti}^F \square \text{Ti}^F \text{Cr}_-^V \text{Ti}^F \square \dots$ is

ultimately realized at $x = \frac{1}{3}$, if the interlayer antiferromagnetic and intralayer ferromagnetic coupling of the magnetic ions is held. This structure has the separated ferromagnetic layers coupled antiferromagnetically ($\text{Cr}_+^V - \text{Cr}_-^V$) and the intralayer ferromagnetic interaction should be predominant. In fact, θ changes from a negative value (-48 K for Cr_3Se_4) to a positive one and reaches a maximum value $+56$ K at $x = \frac{1}{3}$. Below $x = \frac{1}{3}$, θ begins to decrease due to the dilution of magnetic ions in the M^V layer. The predominance of intralayer ferromagnetic coupling is also seen in the behavior of the χ_m vs T curves at lower temperatures for $0.8 \geq x \geq 0.4$; i.e., χ_m abruptly increases at lower temperatures.

On the other hand, as shown in Fig. 7, the variation of the effective magnetic moment P_{eff} shows a break at $x = \frac{2}{3}$, and not at $x = \frac{1}{3}$ where the metal site to be substituted changes from the 2(a) to the 4(i) site. The behavior of P_{eff} can be interpreted on the following assumption. The Cr ions tend to have the Cr^{3+} (d^3) state whether it is situated in the 2(a) site or in the 4(i) site. Therefore, the Cr^{3+} state is stable up to $x = \frac{2}{3}$. However, above this composition, subsequent Cr ions have the Cr^{2+} (d^4) state. Then, finally, an ionic configuration $\text{Cr}^{2+}\text{Cr}_2^{3+}\text{Se}_4^{2-}$ is realized at $x = 1.0$. The compositional variation of P_{eff} based on the above assumption is shown by a broken line in Fig. 7, which can explain the observed behavior qualitatively. It is noteworthy that the valence state of the Cr ions does not correspond to the site it occupies, that is, the site preference cannot be attributed only to a factor such as ionic radii. The strong tendency of the Cr ion for the Cr^{3+} state has also been reported in Cr_xTiSe_2 (20), where the Cr^{3+} state is stable for the wide homogeneity range of the M_3X_4 phase ($0.45 < x < 0.65$).

The site preference of the 3d-transition metal and the magnetic and electric properties in $(M'_x M_{1-x})_3\text{Se}_4$ systems with the Cr_3Se_4

structure including this system are under investigation.

References

1. F. JELLINEK, *Acta Crystallogr.* **10**, 620 (1957).
2. M. CHEVRETON, *Bull. Soc. Fr. Minéral. Cristallogr.* **90**, 592 (1967).
3. M. CHEVRETON AND G. BÉRODIAS, *C. R. Acad. Sci. Paris* **261**, 1251 (1965).
4. G. BÉRODIAS AND M. CHEVRETON, *C. R. Acad. Sci. Paris* **261**, 2202 (1965).
5. R. H. PLOVNIK, M. VLASSE, AND A. WOLD, *Inorg. Chem.* **7**, 127 (1968).
6. M. CHEVRETON AND B. ANDRON, *C. R. Acad. Sci. Paris* **264**, 316 (1967).
7. B. ANDRON, G. BÉRODIAS, M. CHEVRETON, AND P. MOLLARD, *C. R. Acad. Sci. Paris* **263**, 621 (1966).
8. B. ANDRON AND E. F. BERTAUT, *J. Phys. (Paris)* **27**, 619 (1966).
9. K. ADACHI, K. SATO, AND K. KOJIMA, *Mem. Fac. Eng. Nagoya Univ.* **22**, 253 (1970).
10. I. KAWADA AND H. WADA, *Physica B + C* **105**, 223 (1981).
11. M. ISHII, H. WADA, H. NOZAKI, AND I. KAWADA, *Solid State Commun.* **42**, 605 (1982).
12. H. NOZAKI, H. WADA, AND H. YAMAMURA, *Solid State Commun.* **44**, 63 (1982).
13. H. NAKAZAWA, K. TSUKIMURA, H. HIRAI, AND H. WADA, *Acta Crystallogr. B* **39**, 532 (1983).
14. Y. UEDA, K. KOSUGE, M. URABAYASHI, A. HAYASHI, S. KACHI, AND S. KAWANO, *J. Solid State Chem.* **56**, 263 (1985).
15. N. WATANABE, H. ASANO, H. IWASA, S. SATO, H. MURATA, T. FUKIURA, S. TOMIYOSHI, F. IZUMI, AND K. INOUE, KENS Report-V, KEK Progress Report 84-2, p. 581 (1982).
16. F. IZUMI, *J. Crystallogr. Soc. Japan* **27**, 23 (1985) (in Japanese).
17. R. B. VON DREELE, J. D. JORGENSEN, AND C. G. WINDSOR, *J. Appl. Crystallogr.* **15**, 581 (1982).
18. E. F. BERTAUT, G. ROULT, R. ALEONARD, R. PAUTHENET, M. CHEVRETON, AND R. JANSEN, *J. Phys. (Paris)* **25**, 582 (1964).
19. M. YUZURI, *J. Phys. Soc. Japan* **35**, 1252 (1973).
20. N. OHTSUKA, K. KOSUGE, N. NAKAYAMA, Y. UEDA, AND S. KACHI, *J. Solid State Chem.* **45**, 411 (1982).